p53 Accumulation, defective cell proliferation, and early embryonic lethality in mice lacking *tsg101*

Jürgen Ruland*†, Christian Sirard*†, Andrew Elia*†, David MacPherson*†, Andrew Wakeham*†, Limin Li‡, José Luis de la Pompa*†§, Stanley N. Cohen‡, and Tak W. Mak*†¶

*Amgen Institute, 620 University Avenue, †Ontario Cancer Institute, and Departments of Medical Biophysics and Immunology, University of Toronto, Toronto, ON, Canada M5G 2C1; and ‡Department of Genetics, Stanford University School of Medicine, Stanford, CA 94305-5120

Contributed by Stanley N. Cohen, December 4, 2000

Functional inactivation of the tumor susceptibility gene *tsg101* in NIH 3T3 fibroblasts results in cellular transformation and the ability to form metastatic tumors in nude mice. The N-terminal region of tsg101 protein is structurally similar to the catalytic domain of ubiquitin-conjugating enzymes, suggesting a potential role of tsg101 in ubiquitin-mediated protein degradation. The C-terminal domain of TSG101 can function as a repressor of transcription. To investigate the physiological function of *tsg101*, we generated a null mutation of the mouse gene by gene targeting. Homozygous *tsg101*−/− embryos fail to develop past day 6.5 of embryogenesis (E6.5), are reduced in size, and do not form mesoderm. Mutant embryos show a decrease in cellular proliferation *in vivo* and *in vitro* but no increase in apoptosis. Although levels of *p53* transcripts were not affected in *tsg101*−/− embryos, p53 protein accumulated dramatically, implying altered posttranscriptional control of p53. In addition, transcription of the p53 effector, cyclin-dependent kinase inhibitor p21$^{WAF-1/CIP-1}$, was increased 5- to 10-fold, whereas activation of MDM2 transcription secondary to p53 elevation was not observed. Introduction of a *p53* null mutation into *tsg101*−/− embryos rescued the gastrulation defect and prolonged survival until E8.5. These results demonstrate that *tsg101* is essential for the proliferative burst before the onset of gastrulation and establish a functional connection between *tsg101* and the p53 pathway *in vivo*.

The tumor susceptibility gene 101 (*tsg101*) was discovered in mouse fibroblasts by using regulated antisense RNA initiated within a randomly located, chromosomally integrated, retrovirus-based gene search vector (1). Functional inactivation of *tsg101* by antisense transcripts complementary to *tsg101* mRNA leads to transformation of NIH 3T3 cells characterized by colony formation in soft agar and their ability to form metastatic tumors when injected into nude mice (1).

Sequence analysis of *tsg101* cDNA indicates that the gene encodes a 43-kDa protein. Mouse and human TSG101 proteins are 94% identical (2) and contain putative DNA-binding motifs characteristic of transcription factors (1), suggesting that tsg101 may control gene expression. This presumption was supported by the findings that separate domains of *tsg101* can act as transcriptional cofactors that are able to activate or repress nuclear hormone receptor-mediated transactivation (3–5). In addition, the N-terminal region of *tsg101* resembles a group of apparently inactive homologues of ubiquitin-conjugating enzymes, suggesting a possible role for *tsg101* in the regulation of ubiquitin-mediated protein degradation (6, 7). However, the mechanisms by which interference with *tsg101* expression leads to neoplastic transformation remain unknown.

To investigate the physiological role of *tsg101 in vivo*, we generated *tsg101*-deficient mice by gene targeting in embryonic stem cells.

Materials and Methods

Gene Targeting. A genomic DNA clone containing exons 6–10 of *tsg101* was isolated from a 129/J mouse genomic library. A targeting vector was designed to replace a 4.4-kb genomic fragment containing exon 8 and the 5′ part of exon 9 with the PGK*neo* resistance expression cassette in reverse orientation to *tsg101* transcription. The vector was introduced into E14K embryonic stem (ES) cells by electroporation. Cells were subsequently cultured in the presence of 300 μg/ml of G418 (Sigma) for 10 days. Homologous recombinants were identified by PCR and verified by Southern blotting with a PCR-generated 3′ flanking probe containing exon 10 (primer, 5′-AAG TCC AAG AAA GAG AAA AAT and 5′-GGA TTG CTA GAT GCT GTC TGG). ES cell culture and generation of chimeras were performed as described (8). Two independently targeted ES cell clones transmitted the *tsg101* mutation into the germ line.

PCR Analysis of *tsg101* and *p53* Genotypes. Genomic DNA from ES cells, embryos, and neonate tails was isolated and used for PCR or Southern blot analysis as described (8).

tsg101. Primers "c" (5′-CCG TCT GAG GTT GAG TTG TAG) specific for targeted intronic sequence and "d" (5′-GAG AAG GGC TGA GGA GAA ACG) were used to detect the wild-type allele, whereas primers "a" (5′-CGG AAG GCA GTG GTA GAA CCT), specific for sequences in the *neo* resistance gene, and "b" (5′-TAA AGC GCA T GC TCC AGA CTG), derived from the *tsg101* gene downstream of the targeting construct (Fig. 1), were used to detect the recombinant allele.

p53. Primers 5′-GTG TTT CAT TAG TTC CCC ACC TTG AC and 5′-ATG GGA GGC TGC CAG TCC TAA CCC specific for the target sequence in *p53* were used to detect the wild-type allele, whereas primers 5′-GTG GGA GGG ACA AAA GTT CGA GGC C and 5′-TTT ACG GAG CCC TGG CGC TCG ATG T were used for identification of the *p53* recombinant allele.

Histological Analysis. *Tsg101* heterozygous males and females were intercrossed. Deciduae were isolated in ice-cold PBS at day 5.5 of embryogenesis (E5.5), E6.5, and E7.5, fixed overnight in 4% paraformaldehyde at 4°C, dehydrated, and embedded in paraffin. Sections 7 μm thick were cut and stained with hematoxylin and eosin.

***In Situ* Hybridization.** Deciduae were isolated and processed as for histological analysis. The probes used were full-length cDNAs of *tsg101*, *Brachyury* (9), and *HNF-4* (10). Probes were labeled and processed as described (11).

Abbreviations: *tsg101*, tumor susceptibility gene 101; ES, embryonic stem; E*n*, embryonic day *n*; ICM, inner cell mass; cdk, cyclin-dependent kinase.

§Present address: Center for Aging and Developmental Biology, University of Rochester Medical Center, 601 Elmwood Avenue, Box 645, Rochester, NY 14642.

¶To whom reprint requests should be addressed. E-mail: tmak@oci.utoronto.ca.

The publication costs of this article were defrayed in part by page charge payment. This article must therefore be hereby marked "*advertisement*" in accordance with 18 U.S.C. §1734 solely to indicate this fact.

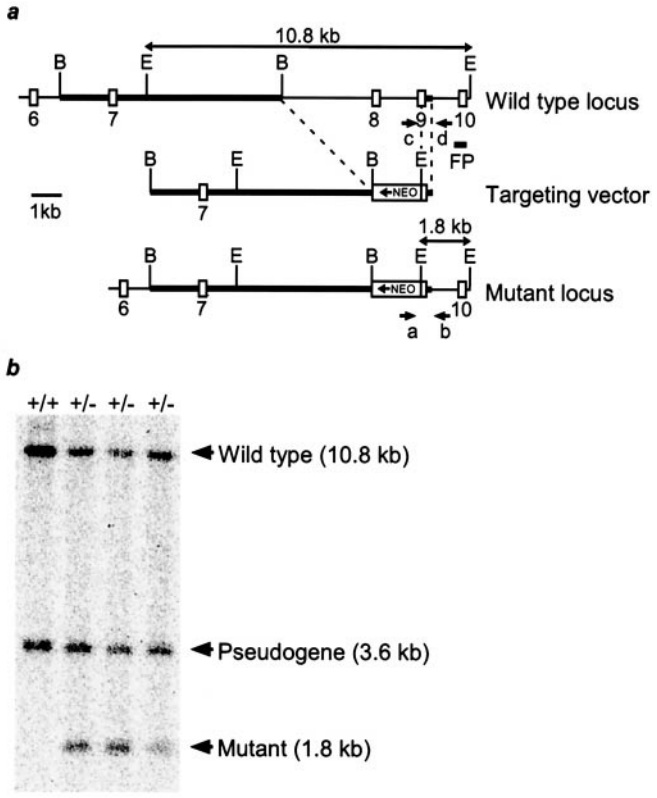

Fig. 1. Targeted disruption of the murine *tsg101* locus. (*a*) Partial genomic organization of the mouse *tsg101* locus (*Top*) and structure of the targeting vector (*Middle*). Coding exons are depicted as open boxes and homologous regions in the targeting vector are indicated by thickened lines. In the mutant allele (*Bottom*), a PGK*neo* cassette replaced 4.4 kb of the *tsg101* locus, encompassing exon 8 and most of exon 9, in opposite orientation to *tsg101* gene transcription. Positions of the PCR primers (*a–d*), 3′ flanking probe (FP) used in Southern blot analysis, and predicted sizes of restriction fragments for genotyping are shown. B, *Bam*HI; E, *Eco*RI. (*b*) Southern blot analysis of ES cell clones generated by homologous recombination at the *tsg101* locus. Genomic DNA from wild-type (+/+) and heterozygous ES cell clones (+/−) was digested with *Eco*RI and hybridized to the indicated 3′ flanking probe. The 1.8-kb fragment is diagnostic of the mutant allele.

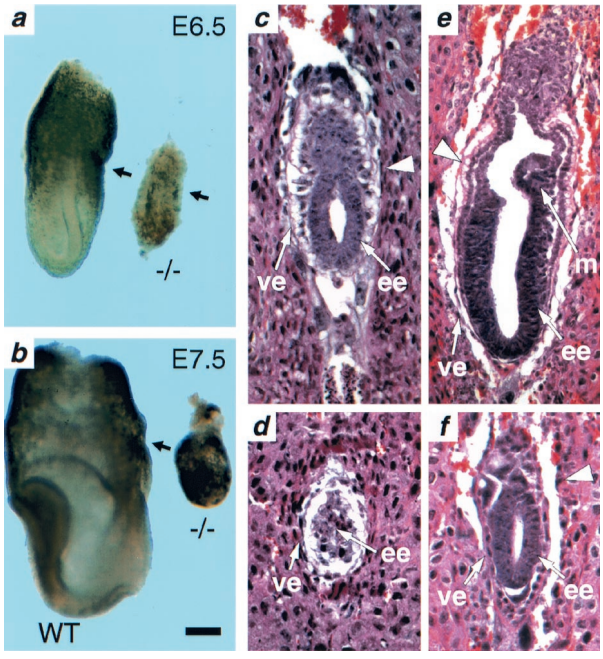

Fig. 2. Severe developmental delay in *tsg101* mutant embryos. Morphology and histological analysis. (*a*) E6.5 *tsg101*−/− embryos (−/−) are smaller and less organized than their wild-type littermates (WT). The arrows point to the separation between the embryonic and extraembryonic regions. (*b*) E7.5 *tsg101*−/− embryos have failed to progress and are starting to be resorbed. (*c*) E5.5 wild-type embryo at the early egg cylinder stage. (*d*) E5.5 *tsg101*−/− embryo showing a poorly defined extraembryonic region and disorganized visceral endoderm. (*e*) E6.5 wild-type egg cylinder stage embryo. Both the embryonic and extraembryonic regions are well-organized and nascent mesoderm tissue can be distinguished. (*f*) E6.5 *tsg101* mutant embryo. The embryonic and extraembryonic regions are severely underdeveloped and no mesoderm is observed. The large arrowhead in *c*, *e*, and *f* points to the separation between the embryonic and extraembryonic regions. ee, embryonic ectoderm; ve, visceral endoderm; m, mesoderm. (Bar = 60 μm in *a*, *c–f*; 120 μm in *b*.)

BrdUrd Labeling of Embryos. BrdUrd labeling of the cells in the S phase of the cell cycle was performed as described (8). BrdUrd (100 mg/g of body weight) was injected i.p. into pregnant females at E6.5. The females were killed 45 min after injection; the deciduae were fixed in 4% paraformaldehyde at 4°C overnight and processed for immunohistochemistry. The sections were incubated with an anti-BrdUrd monoclonal antibody (Roche Molecular Biochemicals) at 1:10 dilution.

***In Vitro* Culture of Preimplantation Embryos.** E3.5 embryos were collected and individually cultured as described (8). Photographs of cultured embryos were taken every 24 h. After 6 days in culture, the morphology of the embryos was recorded and their genotypes were determined by PCR analysis of their DNAs.

Immunohistochemistry. Immunohistochemistry was performed as described (8). Anti-p53 antiserum (NovoCastra, Newcastle, U.K., NCL-p53-CM5p) was used at a 1:200 dilution.

Reverse Transcription–PCR Analysis. Poly(A) RNA was isolated from individual E6.5 embryos by using the MicroFastTrack Kit (Invitrogen). cDNAs were generated by using a cDNA Synthesis Kit (Invitrogen). Quantitative reverse transcription–PCR was performed on cDNAs from single embryos by using specific primers for *p53*, *p21*, *mdm2*, and *β-actin* as described (12). Amplified PCR products were electrophoresed, followed by Southern blotting and hybridization, to a radiolabeled oligonucleotide internal to the amplified product. Signals were quantified by using a PhosphorImager and IMAGEQUANT software (Molecular Dynamics) and normalized to β-actin. One-quarter of the cDNA preparation from each individual embryo was used for genotyping using primers 5′-GGC GGA TGA AGG AGG AAA TG and 5′-GTG GGG CTG TGG GAA TGA TAA and a probe (5′-AAA CTG GAA GAG ATG GTC ACC CGC T) specific for the deleted *tsg101* exons 8 and 9.

Results

Generation and Characterization of *tsg101*−/− Embryos. The murine *tsg101* gene was disrupted by homologous recombination in ES cells (Fig. 1). The mutation was introduced into both C57BL/6J and CD1 genetic backgrounds with no discernable difference in resulting phenotypes. Mice heterozygous for the *tsg101* mutation were phenotypically normal up to 14 mo of age. Heterozygous mice were intercrossed but homozygous *tsg101*−/− neonates were not observed in more than 400 offspring, indicating that homozygous mutation of *tsg101* results in embryonic lethality. To determine the lethality phase of the *tsg101* mutation, embryos from heterozygous intercrosses were analyzed at different days of gestation. At E6.5, approximately 25% of all embryos were phenotypically abnormal. These were genotypically homozygous mutants (Fig. 2*a*). The

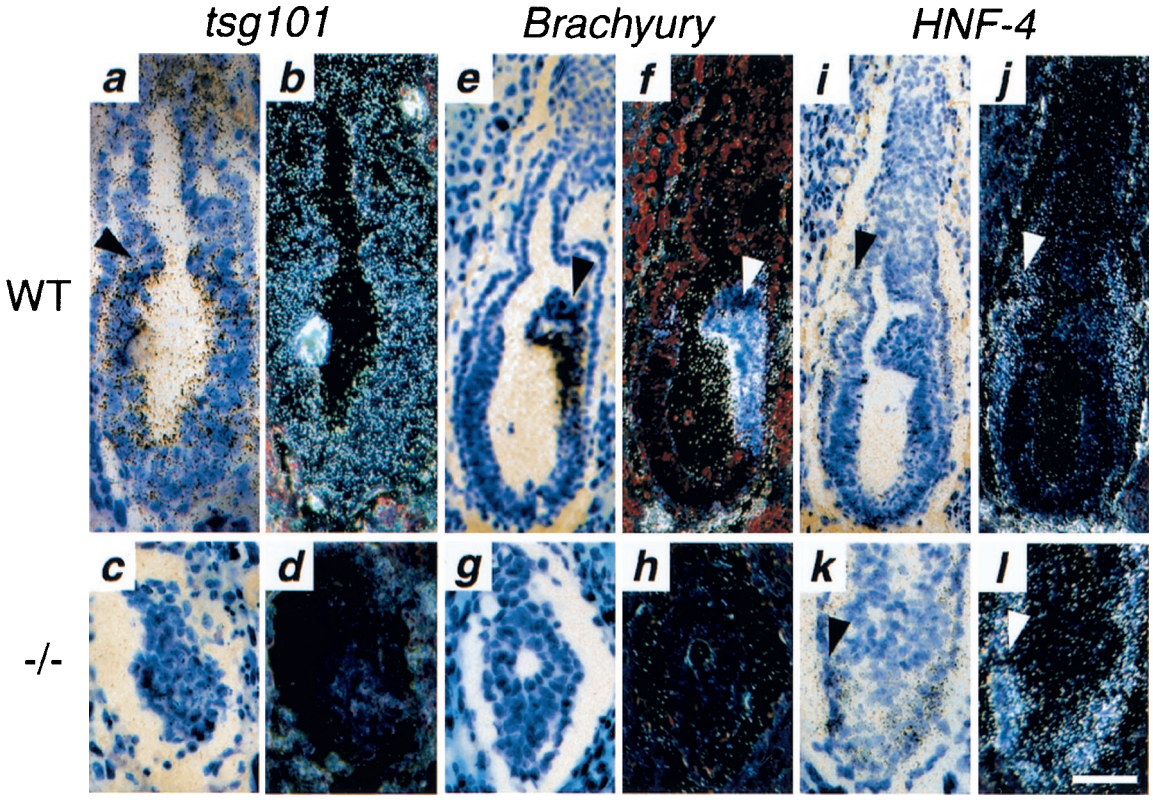

Fig. 3. Spatial expression of *tsg101*, *Brachyury*, and *HNF-4* in E6.5 *tsg101*−/− embryos as determined by *in situ* hybridization: bright-field (*a*, *c*, *e*, *g*, *i*, *k*) and dark-field views (*b*, *d*, *f*, *h*, *j*, and *l*). (*a* and *b*) Ubiquitous *tsg101* expression in sections of a wild-type E6.5 embryo hybridized to an antisense *tsg101* probe. The arrow points to the separation between embryonic and extraembryonic regions. (*c* and *d*) No *tsg101* expression is detected in a *tsg101*−/− E6.5 embryo. (*e* and *f*) *Brachyury* expression in a wild-type E6.5 embryo. Strong expression is detected in the nascent streak (arrow). (*g* and *h*) No *Brachyury* expression is detected in the *tsg101*−/− embryo. (*i* and *j*) *HNF-4* expression in the visceral endoderm (arrow) of a wild-type E6.5 embryo. (*k* and *l*) Normal *HNF-4* expression in a *tsg101*−/− E6.5 embryo. (Bar = 50 μm in *a*–*d*, *g*, *h*, *k*, *l*; 80 μm in e, *f*, *i*, *j*.)

tsg101−/− embryos were smaller than their wild-type littermates and had a poorly defined boundary between the embryonic and extraembryonic regions. At E7.5, mutant embryos had not significantly increased in size or progressed in their development (Fig. 2*b*). By E8.5, most mutant embryos were either in resorption or degenerating within the yolk sac (data not shown). These data indicate that *tsg101* is essential for postimplantation development at the time of initiation of gastrulation.

The structural organization of *tsg101*−/− embryos was characterized in detail by histological analyses of serially sectioned E5.5 and E6.5 embryos obtained from heterozygous intercrosses. Embryos were classified morphologically as wild type or mutant. At the E5.5 egg cylinder stage, wild-type embryos showed a well-organized ectoderm region (Fig. 2*c*), whereas mutant embryos were smaller and poorly organized (Fig. 2*d*). At E6.5, phenotypic differences were even more pronounced. Wild-type embryos exhibited a well-organized ectoderm, visceral endoderm, a primitive streak region, and a developing mesoderm (Fig. 2*e*). In contrast, mutant embryos had no detectable primitive streak, poorly defined visceral and parietal endoderm, and abnormal organization of the extraembryonic region (Fig. 2*f*). Thus, embryos were unable to progress significantly beyond E5.5 in the absence of *tsg101*, a developmental block whose timing coincides with the dramatic increase in embryo size that occurs at E5.5–6.5 during normal mouse development (13).

***Tsg101* Expression and the Effects of Its Absence in Mutant Embryos.** Northern blot analysis showed that *tsg101* transcripts are expressed in wild-type ES cells, throughout normal mouse development, and in all adult tissues analyzed (data not shown; see also refs. 2 and 14). The spatial pattern of *tsg101* expression at E6.5 was analyzed by *in situ* hybridization in tissue sections using a full-length cDNA antisense probe. *Tsg101* expression was ubiquitous in wild-type embryos, detected throughout the epiblast, developing mesoderm, visceral endoderm, extraembryonic ectoderm, and endoderm (Fig. 3 *a* and *b*). No *tsg101* transcripts were detected in mutant embryos (Fig. 3 *c* and *d*), demonstrating that the *tsg101* mutation is a null mutation.

As was shown in Fig. 2*f*, no histological signs of mesoderm formation could be detected in E6.5 *tsg101*−/− embryos. The absence of mesoderm was confirmed at the molecular level by *in situ* hybridization in tissue sections for expression of *Brachyury* (*T*), one of the earliest marker of mesoderm formation expressed at the onset of gastrulation at E6.5 (9). Intense *Brachyury* expression was detected in the nascent primitive streak of wild-type embryos (Fig. 3 *e* and *f*) but not in mutant embryos (Fig. 3 *g* and *h*). In contrast, expression of *Hnf-4*, a transcription factor whose expression is initially restricted to the extraembryonic visceral endoderm (10), was comparable in wild type (Fig. 3 *i* and *j*) and *tsg101*−/− (Fig. 3 *k* and *l*) embryos. Terminal deoxynucleotidyltransferase-mediated UTP end labeling (TUNEL) assays of tissue sections revealed only a few TUNEL-positive nuclei close to the amniotic cavity in both wild-type and mutant embryos, indicating that the reduced size of *tsg101*−/− embryos probably is not caused by an excess of apoptosis (data not shown).

The effect of the *tsg101* mutation on cellular proliferation *in vivo* was examined by BrdUrd incorporation. The ratio of the number of proliferating cells (indicated by BrdUrd-positive nuclei) to the total cell number was taken as the mitotic index. As exemplified in Fig. 4*a*, 70–80% of the nuclei from pheno-

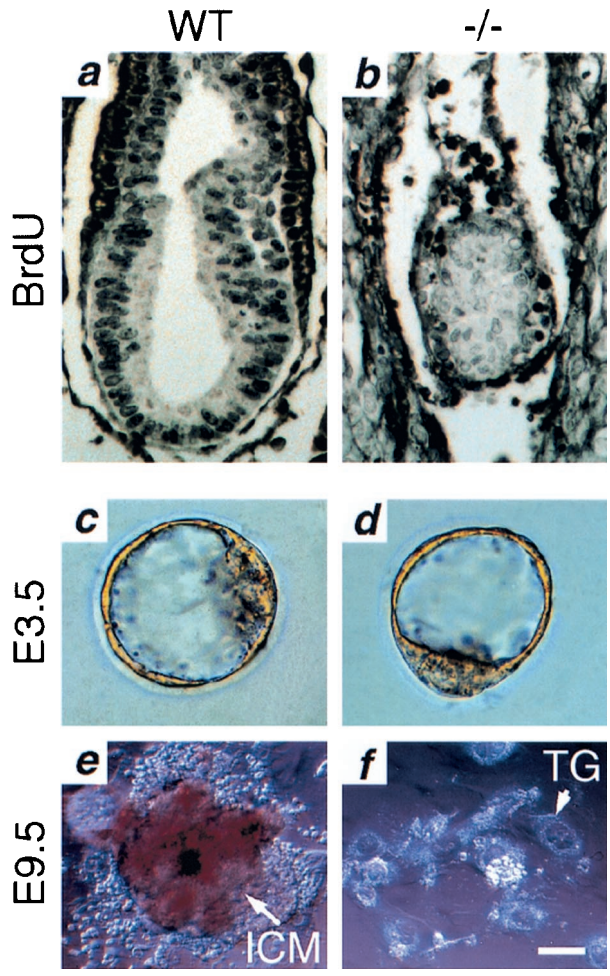

Fig. 4. Reduced cellular proliferation in *tsg101*−/− embryos *in vivo* and *in vitro*. (*a* and *b*) BrdUrd incorporation. (*a*) Strongly BrdUrd-positive nuclei can be seen throughout an E6.5 wild-type embryo. (*b*) Fewer BrdUrd-positive cells with a much weaker signal are seen in an E6.5 *tsg101*−/− embryo. (*c*—*f*) ICM outgrowth. (*c*) Wild-type E3.5 blastocyst. (*d*) *Tsg101*−/− E3.5 blastocyst. (*e*) Wild-type outgrowth after 6 days of culture. The ICM is surrounded by trophoblast giant cells (TG). (*f*) Outgrowth of *tsg101*−/− blastocysts after 6 days of culture. Only TG cells remain. (Bar = 80 μm in *a* and *b*; 20 μm in *c* and *d*; 40 μm in *e* and *f*.)

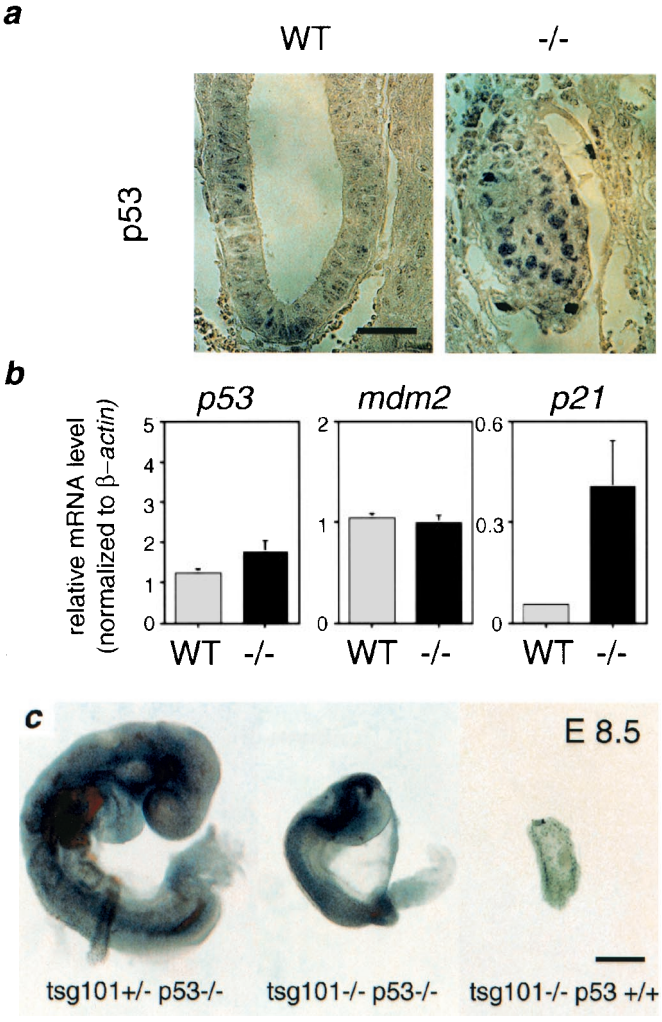

Fig. 5. Deregulated p53 signaling is responsible for the gastrulation defect in *tsg101*−/− embryos. (*a*) Immunohistochemical analysis of p53 protein levels. A few weakly p53-positive cells can be detected in a wild-type E6.5 embryo (WT), whereas strongly p53-positive nuclei occur throughout the *tsg101*−/− embryo (−/−). (Bar = 50 μm.) (*b*) Levels of *p53*, *mdm2*, and *p21* mRNA expression. Quantitative reverse transcription–PCR on mRNA from individual E6.5 wild type (WT) and mutant (−/−) embryos (see *Materials and Methods*). Expression levels are calculated relative to *β-actin*. *p21* expression is increased 5- to 10-fold in *tsg101*−/− embryos. (*c*) Partial rescue of *tsg101*−/− embryos by null mutation of *p53*. Whole mount preparations of embryos from *tsg101*+/−/*p53*+/− intercrosses at E8.5. Although less advanced than their *tsg101*+/−/*p53*−/− littermates (*Left*), *tsg101*−/−/*p53*−/− embryos at E8.5 are developing an anterior–posterior pattern with a head, trunk, and tail region (*Middle*). A remnant of a *tsg101*−/−/*p53*+/+ single mutant embryo at E8.5 is shown on the *Right*. (Bar = 100 μm.)

typically wild-type E6.5 embryos were BrdUrd-positive, producing a mitotic index of 0.7–0.8. However, all mutant embryos analyzed showed <30% nuclear staining (Fig. 4*b*) and a mitotic index of 0.2–0.3. These data indicate that the proliferative capacity of *tsg101*−/− embryos is severely impaired at E6.5 *in vivo*.

To further investigate the growth capability of mutant *tsg101* embryos, E3.5 blastocysts from heterozygous matings were individually cultured *in vitro* (Fig. 4 *c*–*f*). At E3.5, *tsg101*−/− blastocysts were indistinguishable from the wild type (Fig. 4 *c* and *d*), indicating that the *tsg101* mutation does not affect preimplantation development. However, after 6 days in culture, the inner cell mass (ICM) failed to grow in mutant blastocysts, in contrast to extensive ICM proliferation in wild-type blastocysts (Fig. 4 *e* and *f*). In addition, numerous attempts to generate *tsg101*−/− ES cells were unsuccessful (data not shown), further suggesting that a generalized failure of cell cycle progression occurs in the absence of *tsg101*.

Altered Regulation of p53 and Its Effectors in *tsg101*−/− Embryos. Mutations of the *mdm2* protooncogene, whose protein product has ubiquitin ligase activity that negatively regulates the tumor suppressor p53 (15), lead to embryonic lethality before gastrulation with a phenotype resembling that of *tsg101*−/− mutants (16, 17). Mdm2 both represses p53 transcriptional activity and mediates degradation of p53. p53 is capable of blocking cell cycle progression at the G_1 phase through transcriptional upregulation of the cyclin-dependent kinase (cdk) inhibitor $p21^{WAF\text{-}1/CIP\text{-}1}$ (14, 18, 19). Additionally, p53 induces *mdm2* transcription in an autoregulatory feedback loop. Mutational disruption of *mdm2* results in activation and accumulation of p53 (15), generating a proliferative block that leads to early embryonic death around E6.5. However, double mutation of both *p53* and *mdm2* completely rescues this lethality, indicating that accumulation of p53 is the sole cause of the developmental block occurring in *mdm2* mutant embryos (16, 17).

The similar phenotypes observed for both *tsg101* and *mdm2* mutant embryos led us to investigate, by using quantitative reverse transcription–PCR and immunohistochemistry for individual E6.5 embryos, whether the expression of *p53*, *mdm2*, or *p21* was altered in *tsg101*−/− embryos. Immunohistochemical staining showed that, whereas weak anti-p53 staining was observed in a few cells in the epiblast of wild-type embryos, all *tsg101*−/− embryos analyzed showed strong nuclear anti-p53 staining throughout the embryonic and extraembryonic regions (Fig. 5*a*), demonstrating an accumulation of p53 protein. Interestingly, the levels of *p53* and *mdm2* mRNA were unaffected by the absence of *tsg101* (Fig. 5*b*), indicating that the observed p53 accumulation occurs posttranscriptionally, and also indicating the absence of normal *p53* activation of *mdm2* transcription in these embryos. However, with the accumulation of p53 protein, transcription of its downstream effector *p21* was dramatically increased (Fig. 5*b*), suggesting that cell cycle arrest in *tsg101*−/− embryos may result from p53-mediated activation of p21 expression.

To investigate the role of p53 in the lethal block in cell proliferation occurring in *tsg101*−/− mutant embryos, we introduced the *tsg101* mutation into a *p53* null background (20). Sixty embryos from *tsg101*+/−/p53+/− intercrosses in a mixed 129J/C57BL6J/CD1 genetic backgrounds were retrieved at E8.5 and genotyped by PCR. Although no viable tsg101−/− embryos were identified in a p53+/+ or p53+/− background, three tsg101−/− embryos in a p53−/− background were still alive. Although smaller than their wild-type littermates, double mutant embryos developed past the gastrulation stage with a distinct anterior–posterior pattern (Fig. 5*c*). Death of the double mutants occurred between E8.5 and E10.5, indicating a failure of the p53−/− mutation to entirely rescue embryos from the effects of a tsg101 deficiency on development. However, tsg101−/−/p53−/− embryos lived longer and developed further than did tsg101−/− embryos in either a wild-type or p53 heterozygous background, supporting the hypothesis that developmental arrest in early (i.e., E6.5) tsg101−/− embryos is a consequence of p53 accumulation.

Discussion

In this study, we have generated a null mutation in the mouse *tsg101* gene by gene targeting and shown that *tsg101* is required for embryonic cellular proliferation before the onset of gastrulation and for modulation of the *p53* pathway *in vivo*. Tsg101 mutant embryos showed signs of growth retardation as early as E5.5 and did not form mesoderm at E6.5, as revealed by morphological analysis and the absence of *Brachyury* expression. Gastrulation in the mouse embryo occurs at around E6.5 of gestation and requires rapid epiblast proliferation, resulting in a 100-fold increase in cell number between E5.5 and E7.5 (13). *Tsg101*−/− embryos showed reduced BrdUrd incorporation at E6.5, indicating a slowed cell cycle that ultimately culminated in cell cycle arrest and embryonic death. Furthermore, the ICM of *tsg101*−/− blastocysts failed to proliferate *in vitro*, additionally demonstrating a requirement for *tsg101* in embryonic cellular proliferation.

We have shown that accumulation of the tumor suppressor protein *p53* is at least in part responsible for the proliferative block observed in *tsg101*−/− embryos. During normal early mouse development, p53 activation is controlled by its negative regulator Mdm2 in a feedback control loop and p53 is not activated before E11 (21). However, in the absence of *tsg101*, p53 protein accumulates at E6.5 by a posttranscriptional mechanism. This is accompanied by transcriptional upregulation of the p53 target gene *p21*, which is able to block the activity of cyclin-dependent kinases, resulting in slowed progression through the cell cycle (or cell cycle arrest) (18, 19, 22). The elevated transcription of *p21* observed in *tsg101*−/− mutants together with the partial rescue of *tsg101*−/− mutants by deletion of the *p53* gene suggests that the accumulation of p53 and activation of the p53 pathway are responsible for the proliferative block at E6.5 in *tsg101*−/− embryos. However, the subsequent death of *tsg101*−/− embryos at E8.5 indicates that *tsg101* function is also required for other pathways important to later development.

Although our results establish the effect of null mutation of *tsg101* on the p53 pathway, they leave open the possibility that mutation of *tsg101* activates p53 indirectly in early embryos, as occurs following targeted disruption of *Brca1* or *Brca2* (8, 12, 23, 24). *Brca1* and *Brca2* are tumor suppressor genes thought to be involved in the maintenance of genome integrity. *Brca1*−/− and *Brca2*−/− embryos also exhibit a developmental block at gastrulation that is partially rescued by inactivation of p53.

Alternatively, *tsg101* may be directly involved in the regulation of the p53 level *in vivo*. Cellular p53 levels normally are tightly regulated through ubiquitin-mediated proteolysis controlled by the ubiquitin ligase Mdm2 (15). Mdm2 levels are in turn controlled by p53 through feedback regulation and further by modulation of Mdm2 stability itself (25–27). Because of its resemblance to inactive ubiquitin conjugase homologs, it has been speculated that *tsg101* has a role in the regulation of ubiquitin-mediated proteolysis (6, 7), and recently tsg101 has been found to participate with Mdm2 in a feedback control loop that parallels the p53/mdm2 autoregulatory loop (28). Overexpression of *tsg101* inhibits Mdm2 ubiquitination and degradation and consequently decreases the cellular level of p53, whereas elevation of p53 and/or its transcriptionally activated target Mdm2 accelerate decay of *tsg101* (28). These results are consistent with, and complementary to, our *in vivo* findings showing that *tsg101* deficiency results in p53 accumulation, growth arrest, and early embryonic lethality. Additionally, our data show that, in the absence of *tsg101*, p53 accumulation fails to accomplish its normal stimulation of *mdm2* transcription. Thus, the accumulation of p53 observed in *tsg101*−/− embryos may result from at least two separate mechanisms that act at transcriptional and posttranscriptional levels to decrease MDM2-mediated degradation of p53.

We thank Michael Bezuhly, Vincent Tsui, Betty Hum, and Julia Potter for technical assistance; Atsushi Hirao, Razqallah Hakem, and Wen-Chen Yeh for comments and discussion; and Mary Saunders for scientific editing. S.N.C. and L.L. recieved support from the Helmut Horten Foundation and Chiron Corporation. J.R. was supported by a fellowship from the Deutsche Forschungsgemeinschaft.

1. Li, L. & Cohen, S. N. (1996) *Cell* **85,** 319–329.
2. Li, L., Li, X., Francke, U. & Cohen, S. N. (1997) *Cell* **88,** 143–154.
3. Hittelman, A. B., Burakov, D., Iniguez-Lluhi, J. A., Freedman, L. P. & Garabedian, M. J. (1999) *EMBO J.* **18,** 5380–5388.
4. Sun, Z., Pan, J., Hope, W. X., Cohen, S. N. & Balk, S. P. (1999) *Cancer* **86,** 689–696.
5. Watanabe, M., Yanagi, Y., Masuhiro, Y., Yano, T., Yoshikawa, H., Yanagisawa, J. & Kato, S. (1998) *Biochem. Biophys. Res. Commun.* **245,** 900–905.
6. Koonin, E. V. & Abagyan, R. A. (1997) *Nat. Genet.* **16,** 332–333.
7. Ponting, C. P., Cai, Y. D. & Bork, P. (1997) *J. Mol. Med* **75,** 467–469.
8. Hakem, R., de la Pompa, J. L., Sirard, C., Mo, R., Woo, M., Hakem, A., Wakeham, A., Potter, J., Reitmair, A., Billia, F., *et al.* (1996) *Cell* **85,** 1009–1023.
9. Kispert, A. & Hermann, B. G. (1993) *EMBO J.* **12,** 4898–4899.
10. Duncan, S. A., Manova, K., Chen, W. S., Hoodless, P., Weinstein, D. C., Bachvarova, R. F. & Darnell, J. E. J. (1994) *Proc. Natl. Acad. Sci. USA* **91,** 7598–7602.
11. Hui, C. C. & Joyner, A. L. (1993) *Nat. Genet.* **3,** 241–246.
12. Suzuki, A., de la Pompa, J. L., Hakem, R., Elia, A., Yoshida, R., Mo, R., Nishina, H., Chuang, T., Wakeham, A., Itie, A., *et al.* (1997) *Genes Dev.* **11,** 1242–1252.

13. Snow, M. (1977) *J. Embryol. Exp. Morphol.* **42,** 293–303.
14. Wagner, K. U., Dierisseau, P., Rucker, E. B., III, Robinson, G. W. & Hennighausen, L. (1998) *Oncogene* **17,** 2761–2770.
15. Prives, C. (1998) *Cell* **95,** 5–8.
16. Montes de Oca Luna, R., Wagner, D. S. & Lozano, G. (1995) *Nature (London)* **378,** 203–206.
17. Jones, S. N., Roe, A. E., Donehower, L. A. & Bradley, A. (1995) *Nature (London)* **378,** 206–208.
18. el-Deiry, W. S., Tokino, T., Velculescu, V. E., Levy, D. B., Parsons, R., Trent, J. M., Lin, D., Mercer, W. E., Kinzler, K. W. & Vogelstein, B. (1993) *Cell* **75,** 817–825.
19. Gu, Y., Turck, C. W. & Morgan, D. O. (1993) *Nature (London)* **366,** 707–710.
20. Jacks, T., Remington, L., Williams, B. O., Schmitt, E. M., Halachmi, S., Bronson, R. T. & Weinberg, R. A. (1994) *Curr. Biol.* **4,** 1–7.
21. Komarova, E. A., Chernov, M. V., Franks, R., Wang, K., Armin, G., Zelnick, C. R., Chin, D. M., Bacus, S. S., Stark, G. R. & Gudkov, A. V. (1997) *EMBO J.* **16,** 1391–1400.
22. Harper, J. W., Adami, G. R., Wei, N., Keyomarsi, K. & Elledge, S. J. (1993) *Cell* **75,** 805–816.
23. Hakem, R., de la Pompa, J. L., Elia, A., Potter, J. & Mak, T. W. (1997) *Nat. Genet.* **16,** 298–302.
24. Ludwig, T., Chapman, D. L., Papaioannou, V. E. & Efstratiadis, A. (1997) *Genes Dev.* **11,** 1226–1241.
25. Buschmann, T., Fuchs, S. Y., Lee, C. G., Pan, Z. Q. & Ronai, Z. (2000) *Cell* **101,** 753–762.
26. Sherr, C. J. & Weber, J. D. (2000) *Curr. Opin. Genet. Dev.* **10,** 94–99.
27. Zhang, Y., Xiong, Y. & Yarbrough, W. G. (1998) *Cell* **92,** 725–734.
28. Li, L., Liao, L., Ruland, J., Mak, T. W. & Cohen, S. N. (2001) *Proc. Natl. Acad. Sci. USA* **98,** 1619–1624.